ELSEVIER

Chemical Engineering Journal 119 (2006) 71–81

Chemical Engineering Journal

www.elsevier.com/locate/cej

Synthesis and surface modification of ZnO nanoparticles

Ruoyu Hong [a,b,*], Tingting Pan [a], Jianzhong Qian [a], Hongzhong Li [b]

[a] *Department of Chemical Engineering and Key Laboratory of Organic Synthesis of Jiangsu Province, Soochow University, Suzhou 215123, China*
[b] *Key Laboratory of Multiphase Reaction, Institute of Process Engineering, Chinese Academy of Sciences, Beijing 100080, China*

Received 15 September 2005; received in revised form 4 March 2006; accepted 6 March 2006

Abstract

ZnO precursor was prepared by direct precipitation from zinc acetate and ammonium carbonate. ZnO nanoparticles were synthesized by calcination of the precursor at 450 °C for 3 h and the calcination after the heterogeneous azeotropic distillation of the precursor, respectively. The synthesized ZnO nanoparticles were characterized by FT-IR, XRD and TEM. It is concluded that the heterogeneous azeotropic distillation of the precursor effectively reduced the formation of hard agglomerates. The surface modification of synthesized ZnO nanoparticles was conducted by capping with oleic acid, and the existence of organic layer can be confirmed by the FT-IR spectra. The lipophilic degree of surface modified ZnO nanoparticles was measured. The ZnO nanoparticle surface was also modified by SiO_2 coating. The FT-IR spectrum and XPS clearly showed the formation of an interfacial chemical bond between ZnO and SiO_2. In addition, photocatalytic degradation of methyl orange in aqueous solution was performed using ZnO nanoparticles or ZnO/SiO_2 nanoparticles as photocatalyst, respectively. The results showed that the ZnO/SiO_2 nanoparticles have reduced catalytic activity than that of ZnO nanoparticles.

Keywords: ZnO; Nanoparticles; Surface modification; Oleic acid; SiO_2

1. Introduction

Nanosized ZnO has great potentiality for being used in preparing solar cell [1], gas sensors [2,3], chemical absorbent [4,5] varistors [6,7], electrical and optical devices [8–10], electrostatic dissipative coating [11], catalysts for liquid phase hydrogenation [12], and catalysts for photo-catalytic degradation [13–15] instead of titania nanoparticles [16–19]. Hence, investigations on the synthesis and modification of nanosized ZnO have attracted tremendous attentions.

Different synthesis methods have been devised, including sol–gel technique [20,21], microemulsion synthesis [7], mechanochemical processing [22], spray pyrolysis and drying [15,23], thermal decomposition of organic precursor [24], RF plasma synthesis [25], supercritical-water processing [26], self-assembling [27], hydrothermal processing [28,29], vapor transport process [30], sonochemical or microwave-assisted synthesis [31,32], direct precipitation [33] and homogeneous precipitation [34,35].

However, the formation of the bonds of Zn–O–Zn among nanoparticles due to the existence of water molecular results in hard agglomerates, which impede the applications of ZnO nanoparticles. Therefore, removal of water moiety in precursors is a key process for reducing hard agglomerates. Various methods were employed to remove the water in precursors, e.g., the rinse using organic solvent, and this was already adopted in previous research [32,35].

The coating of nanoparticles to enhance the surface chemical and physical properties is the key for the successful applications of nanomaterials. Posthumus et al. [36] modified various oxidic nanoparticles using 3-methacryloxypropyltrimethoxysilane, the compatibility of modified particles with organic matrices was improved. Grasset et al. [37] coated commercial ZnO nanoparticles with aminopropyltriethoxysilane under varying conditions and found that the coating is controllable, the crystallite size remains almost unchanged, the grafting process did not modify the transmittance spectra of ZnO, and the aminosilane coating could increase the photostability. Min et al. [38] deposited conformal Al_2O_3 layer on ZnO nanorods and found that amorphous Al_2O_3 cylindrical shells wrap the ZnO nanorods.

In the present investigation, the precursor of ZnO nanoparticles was prepared by precipitation from the solutions of zinc acetate and ammonium carbonate. ZnO nanoparticles were

* Corresponding author. Tel.: +86 512 6588 0370 (o)/6600 0797 (c); fax: +86 512 6588 0089
E-mail address: rhong@suda.edu.cn (R. Hong).

1385-8947/$ – see front matter © 2006 Elsevier B.V. All rights reserved.
doi:10.1016/j.cej.2006.03.003

obtained after calcination. On one hand, the surface of ZnO nanoparticles was coated with oleic acid to improve the compatibility between inorganic nanoparticles and organic matrix. A covalent bond was formed by chemical reaction between the hydroxylic groups on the surface of ZnO nanoparticles and organic long-chained molecules. On the other hand, the surface of ZnO nanoparticles was coated with silica. An interfacial chemical bond between ZnO and SiO_2 was found, and the catalytic activity of ZnO nanoparticles was greatly reduced.

2. Experimental

2.1. Materials

Zinc acetate ($ZnAC_2{\cdot}2H_2O$), ammonium carbonate ($(NH_4)_2CO_3$), polyethylene glycol (PEG), 1-butanol, *o*-xylene, toluene, ethanol, sulphuric acid (H_2SO_4), $Na_2SiO_3{\cdot}9H_2O$, methyl orange, EtOH and deionized-water were used in the experiments. All the reagents used were analytical grade. The relative molecule weight of PEG is 10,000. The deionized-water was distilled to obtain high-purity water. The distiller was made of quartz and was operated below the boiling point of water.

2.2. Synthesis of nanosized ZnO

$ZnAC_2{\cdot}2H_2O$ and $(NH_4)_2CO_3$ were dissolved in high-purity water to form solutions with certain concentrations, respectively. The two solutions were slowly dropped into the vigorously stirred polyethylene glycol (PEG) solution (5% (w/w), water solution). The precipitate was collected by filtration and rinsed three times with high-purity water and ethanol, respectively. Then the precipitate was dried at 100 °C under vacuum for 12 h to have the precursor ready.

Afterwards the precursor was divided into two parts. One was ball-milled for 1 h and calcinated at 450 °C for 3 h to obtain the ZnO. The obtained powder was ball-milled for 3 h, and was named Powder A.

The other was ball-milled for 1 h and put into 1-butanol according to the weight proportion of the powder to 1-butanol = 1:10. The mixture was dried using heterogeneous azeotropic distillation. The processed precursor was also calcined at 450 °C for 3 h to obtain the ZnO. The obtained powder was ball-milled for 3 h, and was named Powder B.

2.3. Coating with oleic acid

For the surface modification with oleic acid, the amount of oleic acid, reaction time and reaction temperature were varied in the experiments. Typically, oleic acid of 1.5 ml was dissolved in *o*-xylene of 50 ml in a flask to form the solution, and the concentration of the solution is 3%. Powder B of 1 g was then added to the solution to react for 1 h at 50 °C under stirring. The particles were collected by centrifugal separation and washed three times with toluene, then dried under vacuum at 50 °C.

2.4. Coating with SiO_2

Certain amount of ZnO nanoparticles (Powder A) were put into high-purity water in a flask with vigorous agitation to form 20–30% (w/w) slurry. The slurry was vigorously stirred for 45 min, then, was stirred with the aid of ultrasonic oscillation until an excellent dispersion of ZnO nanoparticles was attained. Under strong agitation, the sodium silicate solution was dropped into the flask to set the pH value of slurry to 9.5. The slurry in the flask was heated and maintained at 85–90 °C. Afterwards the sodium silicate solution was dropped again to make the ratio of silica to ZnO to be 2–3% (w/w). Then the pH value was set to 8.5 using dilute sulphuric acid to make the silicic acid deposit on the surface of ZnO nanoparticles. The following chemical reaction took place:

$$NaSiO_3 + H_2SO_4 + (n-1)H_2O = SiO_2{\cdot}nH_2O \downarrow + Na_2SO_4$$

The slurry was maintained at 85–90 °C for 2 h with vigorous agitation. The composite nanoparticles were collected by filtration and rinsed three times with deionized-water, then dried at 100 °C for 12 h.

2.5. Preparation of silica

The sodium silicate solution of 100 ml, which has the same concentration of the solution used in the coating experiment in Section 2.4, was put into a flask, heated and maintained at 85–90 °C. The pH value was set to 8.5 using dilute sulphuric acid. Some colorless siliceous precipitate was formed. The slurry was agitated for 2 h. Then EtOH was dropped to deposit the precipitate. The precipitate was collected by filtration and rinsed three times with deionised-water, then dried at 100 °C for 12 h. The SiO_2 gel was obtained.

2.6. Photocatalysis degradation

The nanoparticles (Powder A) of 0.4 g were put into methyl orange solution of 100 ml with a concentration of 1.25×10^{-3} M. The slurry was magnetically stirred for 20 min, and was put into a photocatalytic apparatus (see Fig. 1). The slurry was under the UV irradiation of a lamp with the power of 30 W. Sampling was taken every hour. The upper lucid liq-

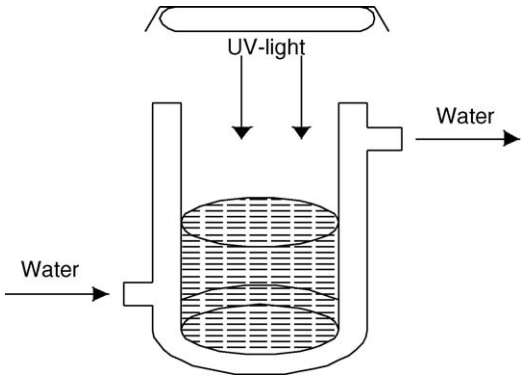

Fig. 1. Experimental apparatus for photo-catalytic degradation.

uid, which was obtained after centrifugal separation, was used to measure the UV–vis absorption. Details about the photocatalysis experiments can be found in Refs. [1,13,19,32,35].

2.7. Measurement of lipophilic degree

The lipophilic degree (LD) of nanoparticles was characterized by dispersing the nanoparticles of 0.5 g in water of 50 ml with the addition of organic solvent [39]. When ZnO nanoparticles were put into water, the uncoated ZnO nanoparticles precipitated in water, while the ZnO nanoparticles which were coated with oleic acid, floated on the water surface. When methanol was dropped into the water slowly and continually with stirring, the modified ZnO nanoparticles were wetted by methanol and hence precipitated gradually. The volume of the methanol used was recorded and the lipophilic degree (LD) was calculated according to the following equation [39]:

$$\mathrm{LD} = \frac{V}{V + 50} \times 100\% \quad (1)$$

where V was the volume of methanol used in the experiments.

2.8. Particle characterization

Fourier transform infrared (FT-IR) analysis was performed using Avatar 360 (Nicolet, USA) with KBr method. X-ray diffraction (XRD) analysis for powders was performed using D/Max-IIIC (Rigaku, Japan) using Cu Kα radiation. The size and shape of nanoparticles were determined using a high-resolution transmission electron microscope (HRTEM, JEM-2010, Jeol, Japan) and a transmission electron microscope (TEM, H-600-II, Hitachi, Japan). The nanoparticle morphology was measured using a scanning electronic microscope (SEM S570, Hitachi, Japan). The UV–vis absorption of methyl orange solution was measured using a U-2810 spectrophotometer (Hitachi, Japan).

X-ray photoelectron spectra (XPS) measurements of synthesized ZnO and SiO_2-coated ZnO nanoparticles were carried out with the Al Kα line as the excitation source ($h\nu = 1486.6$ eV) using a PHI 5000C (Perkin-Elmer, USA). The background pressure was less than 2×10^{-9} Torr. The binding energies were referenced to the C 1s line at 284.6 eV with an uncertainly of ±0.2 eV.

3. Results and discussion

3.1. Comparison of two synthesis routes for ZnO

3.1.1. FT-IR spectra

Fig. 2a and b show the FT-IR absorption spectra of the precursor, and the precursor after heterogeneous azeotropic distillation with 1-butanol, respectively. In Fig. 2b, the peak at 2900–3000 cm^{-1}, which did not appear in Fig. 2a, can be attributed to the symmetric and asymmetric vibrations of $–CH_2–$ and $–CH_3$ groups, indicating that the particles of precursor are surrounded by the molecules of 1-butanol.

3.1.2. XRD patterns

The XRD patterns of ZnO nanoparticles are illustrated in Fig. 3. All peaks can be well indexed to the zincite phase of ZnO (International Center for Diffraction Data, JCPDS 36-1451). No peaks from other phase of ZnO and impurities are observed, suggesting that high-purity ZnO be obtained. In addition, all peaks of the ZnO nanoparticles (Powder A) are higher than those (Powder B) synthesized by heterogeneous azeotropic distillation. Moreover, the peak width of half-maximum height of Powder B is also wider, implying that the heterogeneous azeotropic distillation tends to reduce the integrity of crystalline structure. The ZnO particle diameter D was calculated using the Debye–Sherrer formula $D = K\lambda/(\beta \cos\theta)$, where K is Sherrer constant, λ is the X-ray wavelength, β is the peak width of half-maximum, and θ is the Bragg diffraction angle. The XRD peaks give the diameter of about 40 nm for Powder A and about 30 nm for Powder B, and are basically in accordance with the TEM images shown in the next section.

3.1.3. TEM images

Fig. 4 illustrates the TEM images of Powder A and Powder B. As shown in Fig. 4b, Powder B consists mainly of spherical particles of a size about 30 nm. In Fig. 4a, the particles of Powder A aggregated severely. Moreover, it can be seen that the particle size of Powder A is larger than that of Powder B. This indicates that the heterogeneous azotropic distillation process dehydrated the most water of precursor and avoided the hard aggregation of nanoparticles.

3.1.4. Dispersion of powders

In this section, four kinds of nano-suspensions were prepared, which might be used to prepare nano-coatings. Powder A, Powder B, surface-modified Powder A and surface-modified Powder B (surface modification with oleic acid, see Section 2.3) were added, respectively into acetone, then PEG (0.5% concentration in weight) was added. The mixtures with a solid weight concentration of 5% were ball-milled for 1 h to prepare nano-suspensions.

To compare the difference of four kinds of nanoparticles, the sedimentation behaviors of nano-suspensions were compared [40]. The results showed a remarkable difference. The first nano-suspension (with Powder A) will precipitate at a higher rate, while the fourth one (with surface-modified Powder B) gives a stable colloid in acetone. The averaged sedimentation rate (R) of particles is 11.5, 6.78, 5.65 and 2.29 mm/d, respectively, indicating that the dispersion of Powder B is much better than that of Powder A, moreover, surface modification with oleic acid further increases the dispersion of nanoparticles.

3.2. Coating with oleic acid

3.2.1. FT-IR spectra

Fig. 5a and b show the FT-IR spectra of oleic acid-capped ZnO nanoparticles and Powder B, respectively. Comparing the spectra of Powder A (Fig. 5a) with that of Powder B (Fig. 5b), the stretching vibrations of the −OH group of oleic acid-capped ZnO nanoparticles and Powder B are observed at −3406 cm^{-1}

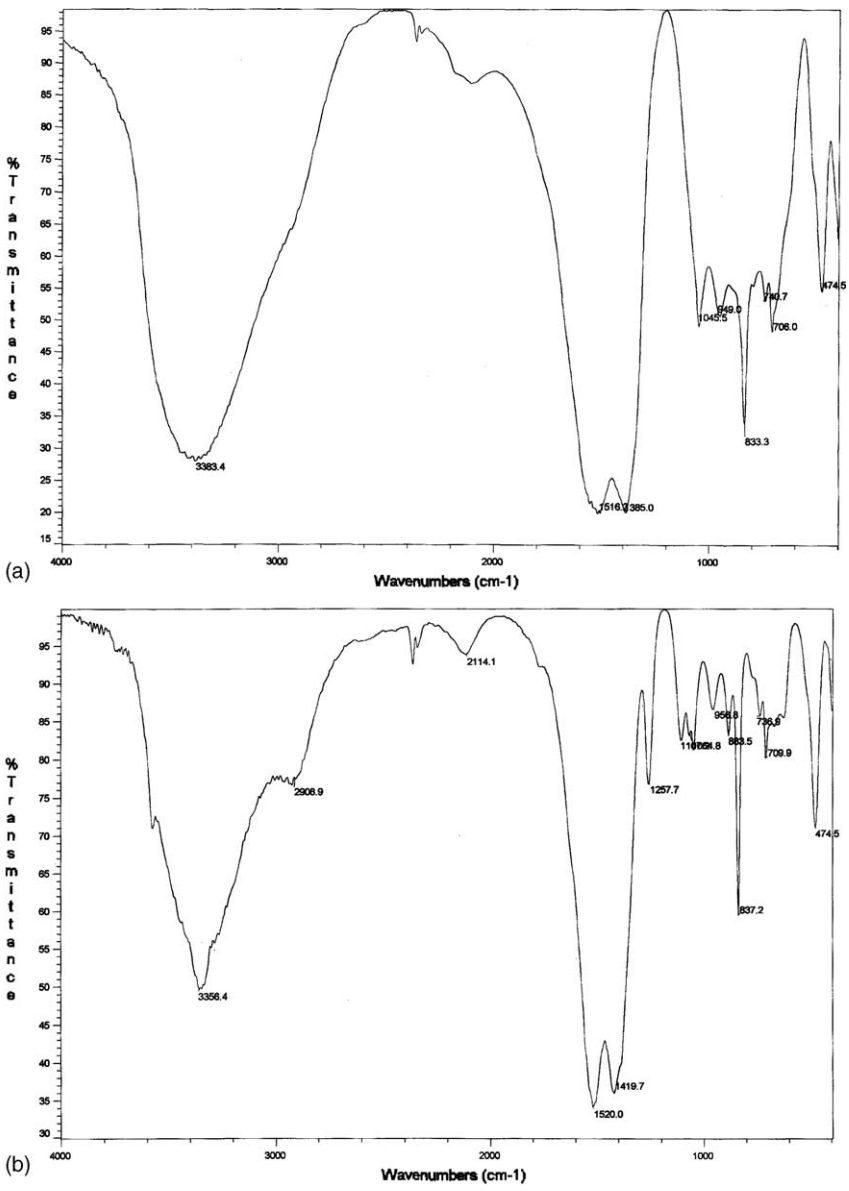

Fig. 2. FT-IR spectra of (a) the precursor and (b) the precursor after heterogeneous azeotropic distillation with 1-butanol.

(Fig. 5a) and ~3449 cm^{-1} (Fig. 5b), respectively. However, peaks at ~2924 and ~2854 cm^{-1} in Fig. 5a are attributed to the asymmetric and symmetric stretching vibrations of $-CH_2$ group, which are not observed in Fig. 5b. Furthermore, the peaks at ~1577 cm^{-1} in Fig. 5a are attributed to the stretching vibrations of COO–Zn, implying that the −COOH group of the oleic acid and the −OH group on the surface of ZnO nanoparticles have conducted the following reaction:

$$ZnO(OH)_x + yHOOC(CH_2)_7CH{=}CH(CH_2)_7CH_3 \rightarrow +ZnO(OH)_{x-y}[OOC(CH_2)_7CH{=}CH(CH_2)_7CH_3]_y + yH_2O$$

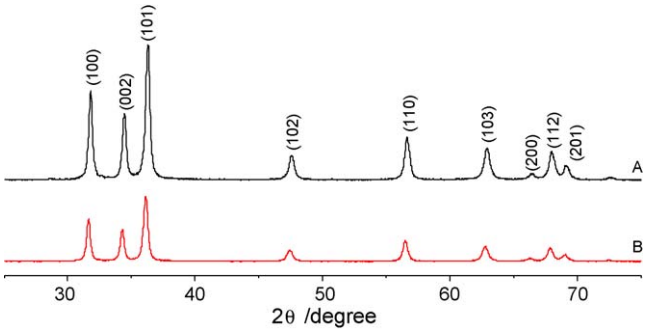

Fig. 3. X-ray powder diffraction patterns of Powder A (A) and Powder B (B).

The peaks at 1725–1700 cm^{-1}, which are due to the stretching vibrations of the C=O group of the free oleic acid, do not appear in Fig. 5a. This suggests that a monomolecular layer on nano-sized ZnO surface be formed. A proposed structural model for oleic acid-capped ZnO nanoparticles is illustrated in Fig. 6.

ZnO nanoparticles (Powder A or Powder B) can stably suspend in polar solvent, e.g., water, but not in non-polar solvent

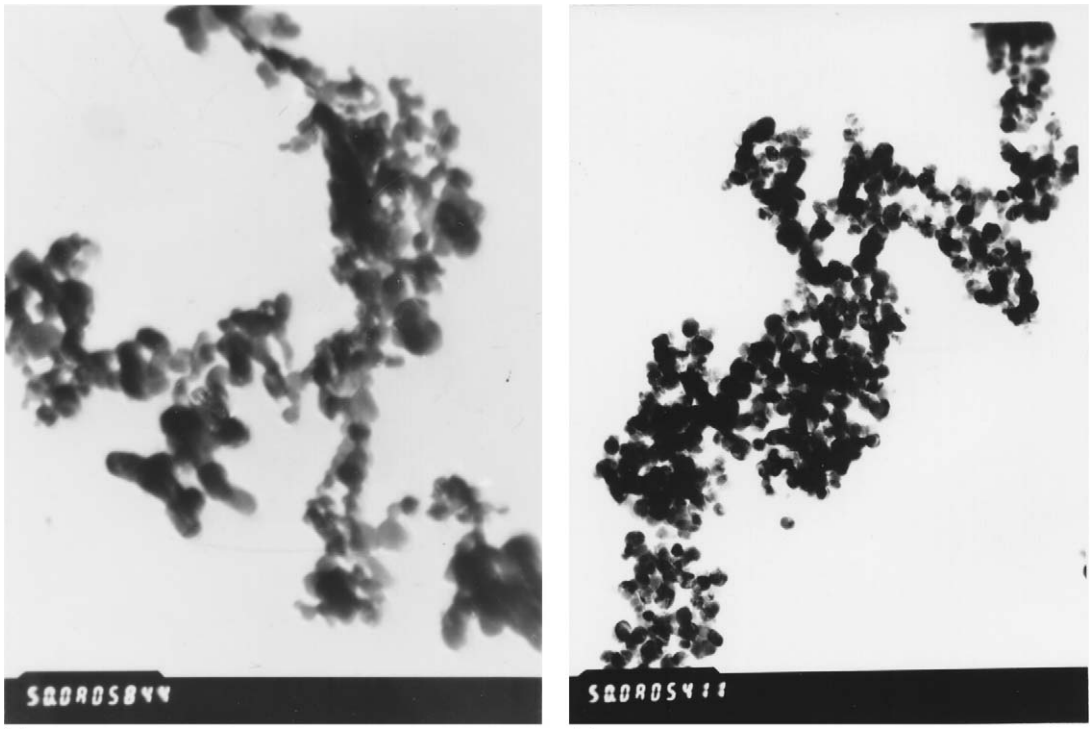

(a) (b)

Fig. 4. TEM images of Powder A (a) and Powder B (b).

such as *n*-hexane. This indicates that these ZnO nanoparticles are polar. However, the ZnO nanoparticles modified by oleic acid were observed to float on the surface of water, and stably suspend in *n*-hexane. This indicates that the nanosized ZnO powder is varied from polarity to non-polarily after the surface of nanoparticles capped by a monomolecular layer of oleic acid. The lipophilic degree (LD) of synthesized ZnO nanoparticles (Powder B) were measured using the method explained in Section 2.7.

Meanwhile, the molecules of 1-butanol capped on particle surface prevented nanoparticles from aggregating and coarsening at some extent.

3.2.2. XRD patterns

XRD patterns of ZnO nanoparticles before and after surface coating with oleic acid are similar. All peaks can be well indexed to the zincite phase of ZnO.

3.2.3. SEM images

The SEM images of the ZnO nanoparticles (Powder B) and the oleic acid-capped ZnO nanoparticles are shown in Fig. 7a and b. From Fig. 7b, it is confirmed that the morphology of the oleic acid-capped ZnO nanoparticles (Fig. 7b) is close to that of the ZnO nanoparticles (Powder B, shown in Fig. 7a).

3.2.4. Lipophilic degree (LD)

Factors influencing the lipophilic degree (LD) are: the concentration of oleic acid, the reaction temperature and the reaction time. These factors are varied in the experiments, and the measured LDs are illustrated in Fig. 8.

3.2.4.1. Influence of oleic acid concentration. The influence of oleic acid concentration (wt.%) on LD is illustrated in Fig. 8a. As shown in Fig. 8a, the LD increases with the increasing oleic acid concentration when the oleic acid concentration is less than 5%; when the concentration increases above 5%, the LD decreases. This indicates that oleic acid reaches the saturation of single-molecular-layer adsorption when concentration $C = 5\%$, and higher concentration of oleic acid has no effect to improve the LD. When the oleic acid concentration increases further, the long chain of oleic acid entangles with each other, and hinders the carboxyl group (−COOH) of the oleic acid to react with the hydroxide group on the surface of ZnO nanoparticles.

3.2.4.2. Influence of reaction temperature. The influence of reaction temperature on LD is illustrated in Fig. 8b. As shown in Fig. 8b, the LD increases with the increasing temperature when the reaction is lower than 50 °C, and reaches its maximum at 50 °C. It means that the single-molecular-layer adsorption reaches its equilibrium at the reaction temperature of 50 °C.

3.2.4.3. Influence of reaction time. Fig. 8c shows that when the reaction time reaches $t = 1$ h, the LD does not increase obviously. The single-molecular-layer adsorption reaches its equilibrium at the reaction time $t = 1$ h. Therefore, the optimal reaction time is 1 h.

3.3. Coating with silica

3.3.1. XRD spectrum

The XRD spectra of ZnO nanoparticles coated with SiO_2 are in accordance with those of pure ZnO nanoparticles which

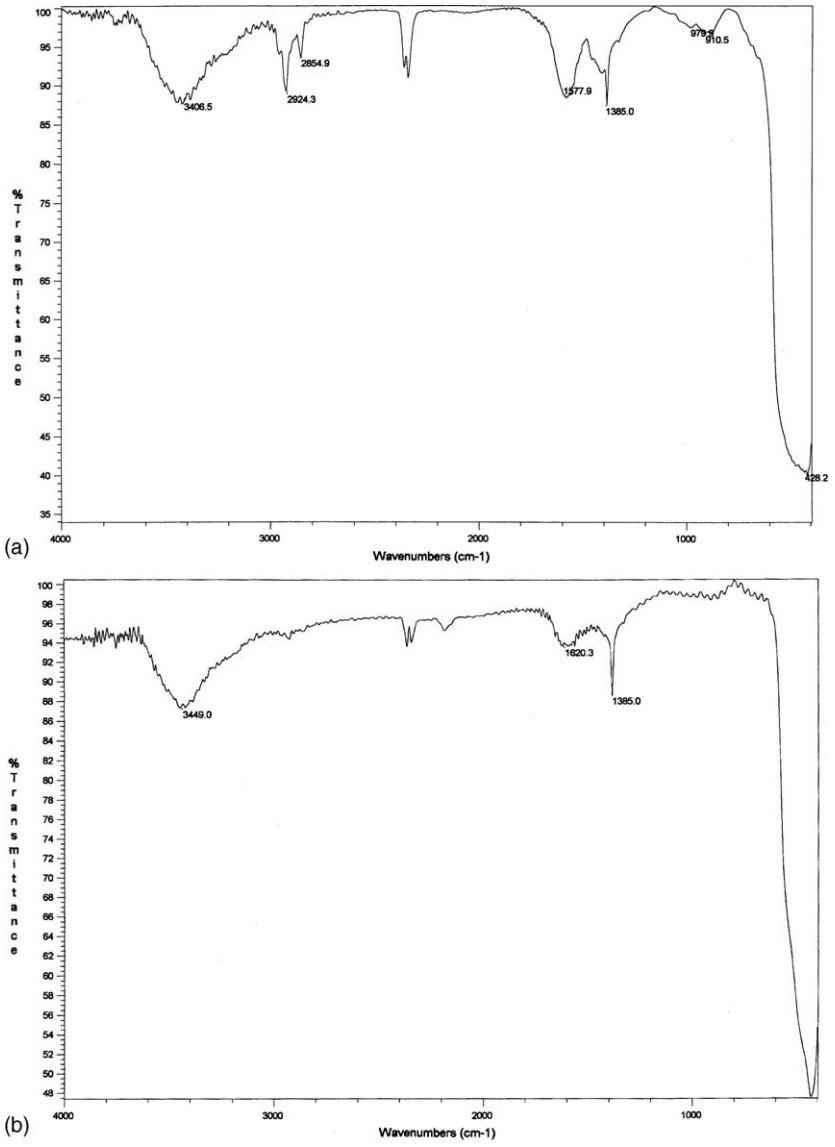

Fig. 5. FT-IR spectrums of oleic acid-capped ZnO nanoparticles (a) and Powder B (b).

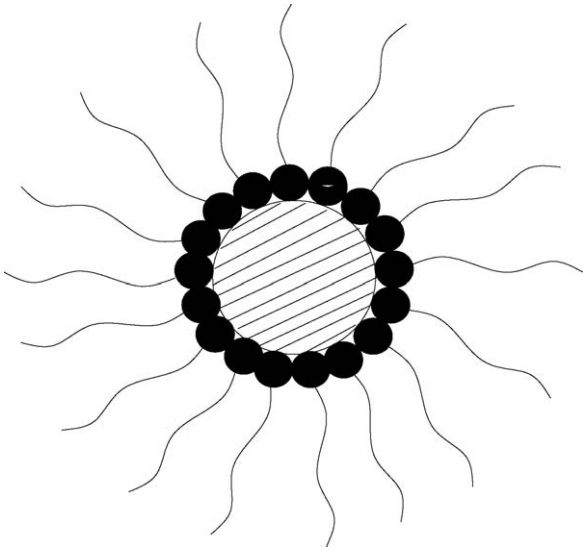

Fig. 6. Aproposed structural model for oleic acid-capped ZnO nanoparticles.

were shown in Fig. 3. This is due to the fact that the SiO_2 obtained by the hydrolysis of sodium silicate is amorphous. The diffraction patterns of the amorphous SiO_2 are very weak, as shown in Fig. 9, which can be easily covered by the patterns of ZnO.

3.3.2. *HRTEM images*

Fig. 10a is the HRTEM images of synthesized ZnO nanoparticles. As shown in Fig. 10a, the diameters of ZnO nanoparticles are about 35–40 nm, and are in accordance with the prediction from Debye–Sherrer formula given in Section 3.1.2 and TEM images in Section 3.1.3. There is some agglomeration among nanoparticles.

Fig. 10b is the HRTEM images of ZnO/SiO_2 composite nanoparticles. The dispersibility and uniformity of the coated ZnO nanoparticles are better than those of the uncoated ones. The coating technology using SiO_2 thin film on ZnO nanoparticles could reduce the agglomeration among nanoparticles.

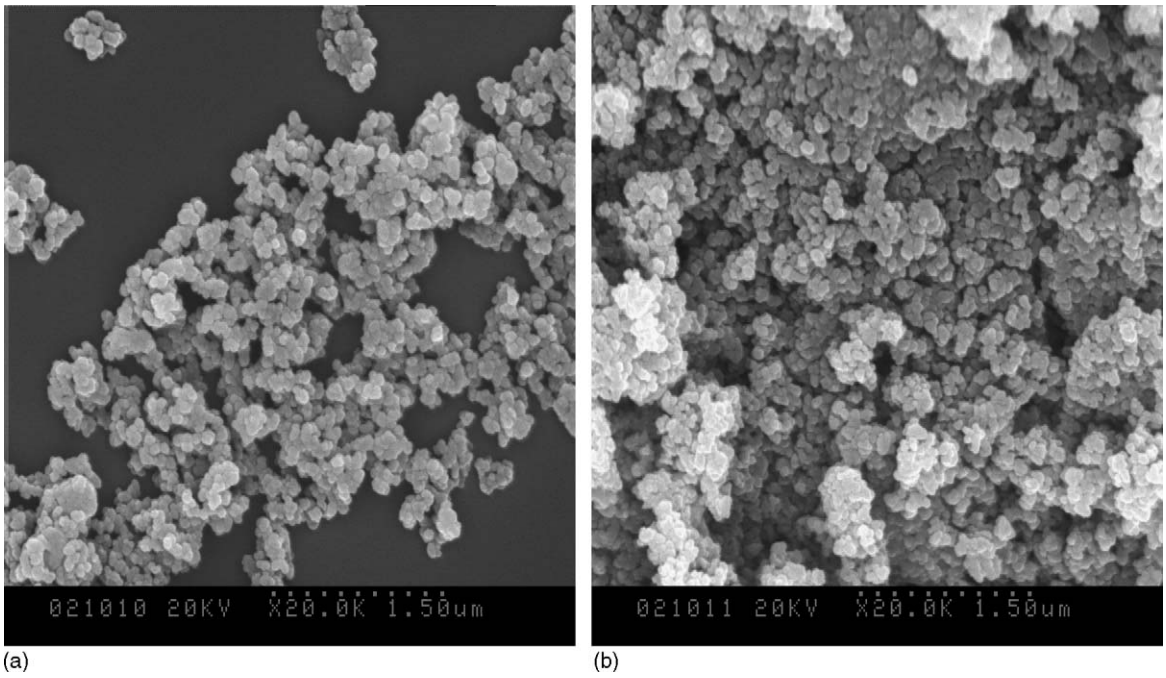

Fig. 7. SEM images of nano sized ZnO (Powder B, (a)) and oleic acid-capped ZnO nanoparticles (b).

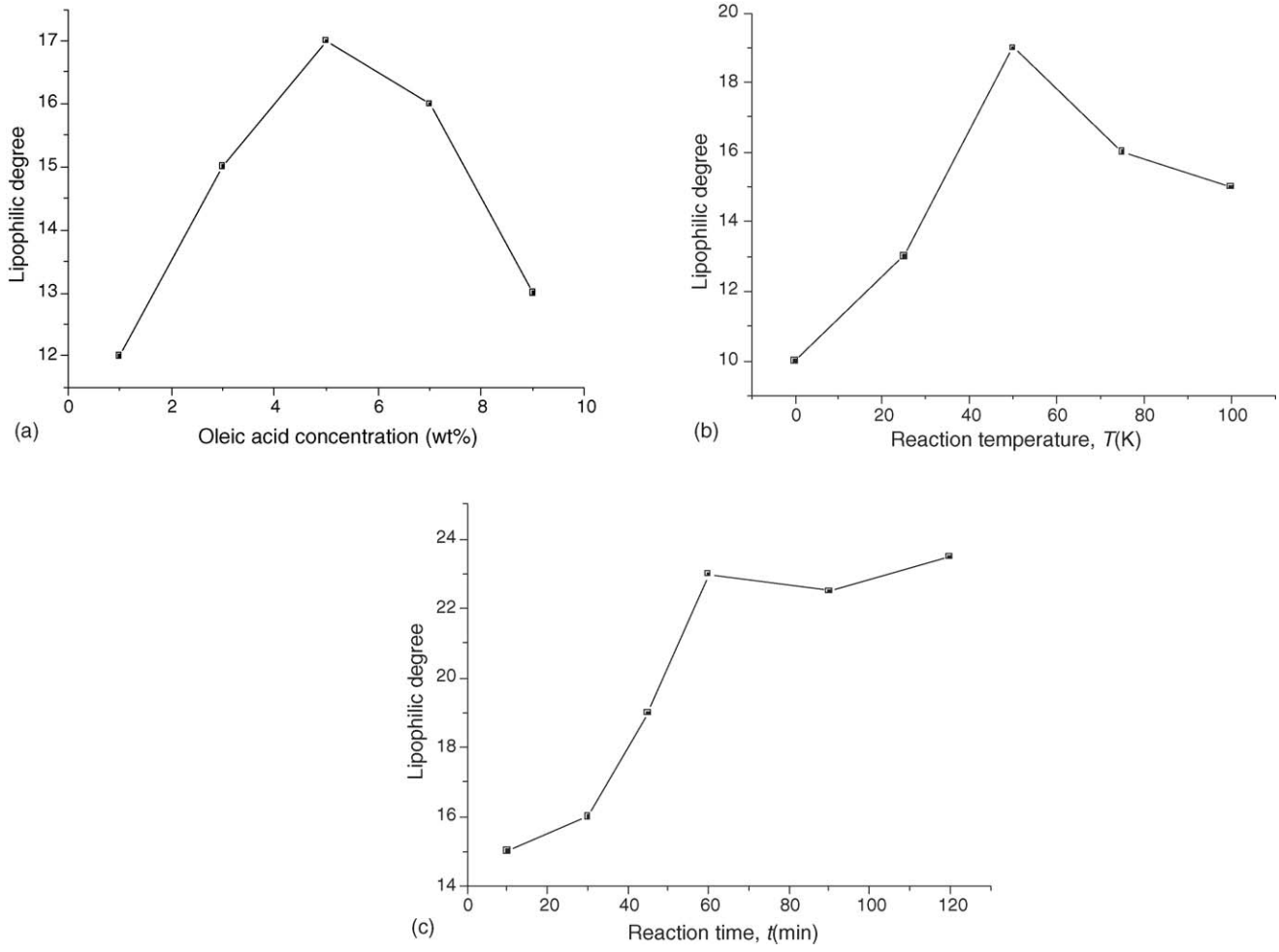

Fig. 8. Influence of leaction time, temperature and oleic acid concentration on modification effect. (a) LD vs. oleic acid concentration ($t = 50$ min, $T = 40\,^{\circ}$C). (b) LD vs. reaction temperature ($C = 5\%$, $T = 50$ min). (c) LD vs. reaction time ($C = 5\%$, $T = 50\,^{\circ}$C).

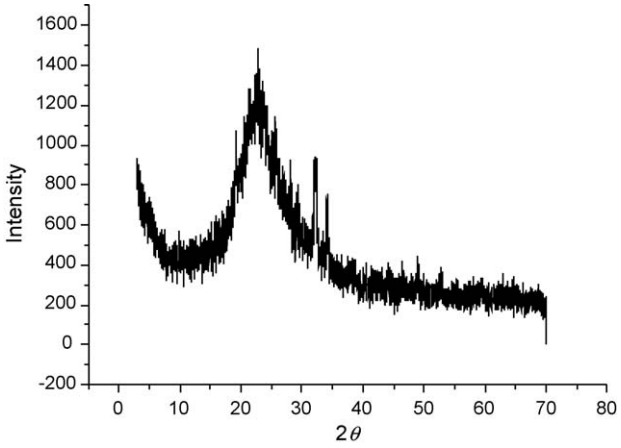

Fig. 9. X-ray powder diffraction patterns of SiO_2.

3.3.3. SEM images

Comparing the SEM images of nanoparticles before and after coating with SiO_2, as shown in Fig. 7a, Fig. 7b and Fig. 11, it is found that the dispersibility of the nanoparticles was improved after coating with SiO_2. Similar phenomenon was revealed by the HRTEM images in the previous section.

3.3.4. FT-IR spectra

Fig. 12 is the FT-IR absorption spectrum of nanoparticles after coating with SiO_2. By comparing Fig. 12 with Fig. 5b, it could be found that for the ZnO nanoparticles coated with SiO_2 there is a new absorption peak at 979.9 cm^{-1}, which can be attributed to the flex vibrations of Si–O–Zn. It demonstrated that ZnO nanoparticles connects SiO_2 thin film with chemical bond. The amorphous hydrated silica combines firmly onto the surface of ZnO nanoparticles with hydroxyl to form ZnO/SiO_2 composite nanoparticles.

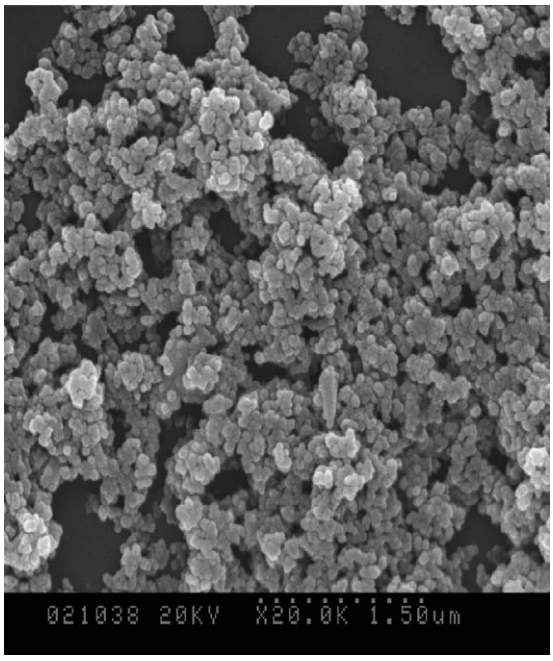

Fig. 11. SEM image of synthesized ZnO/SiO_2.

3.3.5. XPS spectra

Fig. 13 is the XPS spectra of synthesized ZnO and SiO_2-coated ZnO nanoparticles. Comparing the XPS spectrum of ZnO with that of ZnO/SiO_2, it can be seen that there exists the peak at 103 eV corresponding to the binding energy of Si 2p. The binding energy of element Si is about 97 eV. This illustrates that the surface of ZnO nanoparaticles is coated with SiO_2. The result also agrees with the FT-IR analysis.

The XPS test also shows the atomic contents within 10 nm of the nanocomposite surface: Zn 26.3%, Si 12.9% and O 60.8%. This proves that the contents of the nanocomposite surface are ZnO and SiO_2.

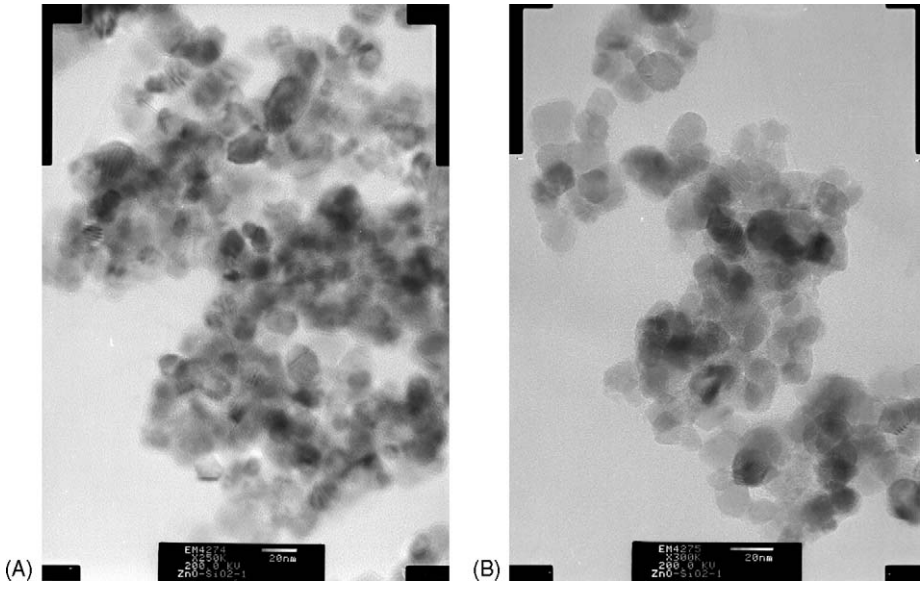

Fig. 10. HRTEM images of Powder A (a) and composite nanoparticles (b)(a) HRTEM image of synthesized ZnO. (b) HRTEM image of synthesize ZnO/SiO_2.

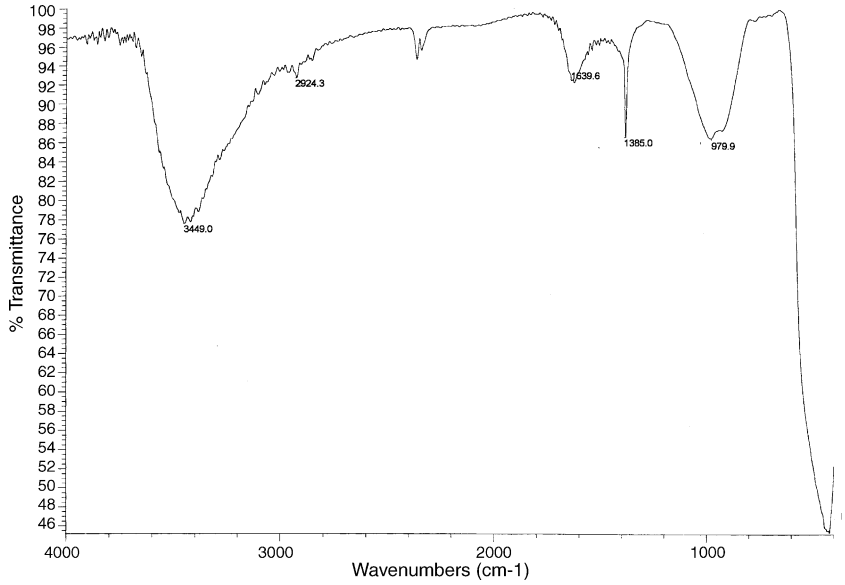

Fig. 12. FT-IR spectra of ZnO/SiO_2.

3.3.6. Reduction of photocatalytic activity

ZnO nanoparticles and ZnO/SiO_2 composite nanoparticles were used as photocatalysts respectively to degrade methyl orange dissolved in water. Fig. 14 shows the UV–vis absorption of methyl orange solution after some time under UV irradiation. It could be seen that the original ZnO nanoparticles have high photocatalytic activity, while the activity was greatly reduced if the surface of ZnO nanoparticles was coated with SiO_2. The photocatalysis experiment also implied that a thin film of SiO_2 was formed on the surface of ZnO nanoparticles to reduce the photocatalytic properly of ZnO nanoparticles. This agrees with the FT-IR and XPS analyses.

It can be easily understood that, the SiO_2 film on the particle surface does not possess photocatalytic capability and will not generate the couple of void and electron under UV irradiation. Although the inner of the nanoparticles is quite active and might generate the couple of void and electron under UV irradiation, some generated void or electron cannot move to the particle surface and hence will not contact the aqueous solution. Therefore, the photocatalytic property of ZnO nanoparticles was reduced.

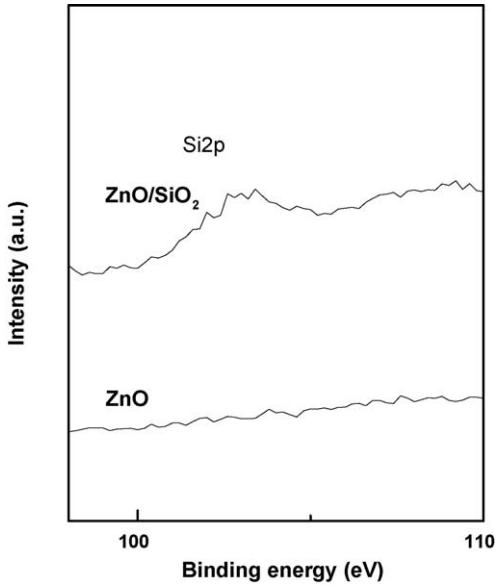

Fig. 13. XPS spectra of ZnO and ZnO/SiO_2.

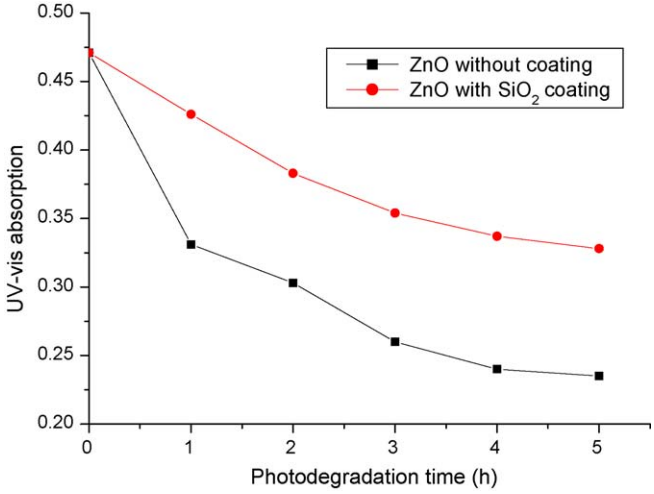

Fig. 14. UV–vis absorption of methyl orange solution vs. time using ZnO (Powder A) and ZnO/SiO_2, respectively.

4. Conclusions

The nanosized ZnO powders were synthesized by two different routines. The obtained nanoparticles were coated with oleic acid or SiO_2, respectively. The following conclusions can be drawn from our experiments and analyses.

(1) Heterogeneous azeotropic distillation of precursor could reduce the integrity of crystalline structure of ZnO, avoid hard aggregation and reduce the average particle size.

(2) The oleic acid-capped ZnO nanoparticles were obtained by the reaction between −OH group on the nanoparticles and −COOH of the oleic acid. FT-IR results confirm that an organic layer exists and the linkage between inorganic nuclei and organic layer is chemical bond. The mechanism of organo-capped ZnO nanoparticles was proposed. In addition, the LD of ZnO nanoparticles was measured.
(3) The ZnO surface was coated with amorphous silica thin film. The coating on the surface of ZnO nanoparticles could successfully improve the dispersibility and hence reduce the agglomeration of nanoparticles. Without coating, the photocatalytic activity of the synthesized ZnO nanoparticles is high. With surface coating by SiO_2, the photocatalytic activity is greatly reduced.

Acknowledgments

The project was supported by the National Natural Science Foundation of China (NNSFC, No. 20476065), the Scientific Research Foundation for the ROCS of State Education Ministry (SRF for ROCS, SEM), the Key Laboratory of Multiphase Reaction of the Chinese Academy of Science (No. 2003-5), and the Key Laboratory of Organic Synthesis of Jiangsu Province.

References

[1] Z.S. Wang, C.H. Huang, Y.Y. Huang, Y.J. Hou, P.H. Xie, B.W. Zhang, H.M. Cheng, A highly efficient solar cell made from a dye-modified ZnO-covered TiO_2 nanoporous electrode, Chem. Mater. 13 (2001) 678–682.
[2] H.M. Lin, S.J. Tzeng, P.J. Hsiau, W.L. Tsai, Electrode effects on gas sensing properties of nanocrystalline zinc oxide, Nanostruct. Mater. 10 (1998) 465–477.
[3] J.Q. Xu, Q.Y. Pan, Y.A. Shun, Z.Z. Tian, Grain size control and gas sensing properties of ZnO gas sensor, Sens. Actuators B -Chem. 66 (2000) 277–279.
[4] R. Turton, D.A. Berry, T.H. Gardner, A. Miltz, Evaluation of zinc oxide sorbents in a pilot-scale transport reactor: sulfidation kinetics and reactor modeling, Ind. Eng. Chem. Res. 43 (2004) 1235–1243.
[5] I. Rosso, C. Galletti, M. Bizzi, G. Saracco, V. Specchia, Zinc oxide sorbents for the removal of hydrogen sulfide from syngas, Ind. Eng. Chem. Res. 42 (2003) 1688–1697.
[6] J. Wu, C.S. Xie, Z.K. Bai, B.L. Zhu, K.J. Huang, R. Wu, Preparation of ZnO–glass varistor from tetrapod ZnO nanopowders, Mater. Sci. Eng. B 95 (2002) 157–161.
[7] M. Singhal, V. Chhabra, P. Kang, D.O. Shah, Synthesis of ZnO nanoparticles for varistors application using Zn-substituted aerosol of microemulsion, Mater. Res. Bull. 32 (1997) 239–247.
[8] C. Feldmann, Polyol-mediated synthesis of nanoscale functional materials, Adv. Fundam. Mater. 13 (2003) 101–107.
[9] M.J. Zheng, L.D. Zhang, G.H. Li, W.Z. Shen, Fabrication and optical properties of large-scale uniform zinc oxide nanowire arrays by one-step electrochemical deposition technique, Chem. Phys. Lett. 363 (2002) 123–128.
[10] R. Wu, C.S. Xie, Formation of tetrapod ZnO nanowhiskers and its optical properties, Mater. Res. Bull. 39 (2004) 637–645.
[11] M. Kitano, M. Shiojiri, Benard convection ZnO/resin lacquer coating—a new approach to electrostatic dissipative coating, Powder Technol. 93 (1997) 267–273.
[12] G.M. Hamminga, G. Mul, J.A. Moulijn, Real-time in situ ATR-FTIR analysis of the liquid phase hydrogenation of γ-butyrolactone over Cu–ZnO catalysts: a mechanistic study by varying lactone ring size, Chem. Eng. Sci. 59 (22–23) (2004) 5479–5485.
[13] M.L. Curridal, R. Comparelli, P.D. Cozzli, G. Mascolo, A. Agostiano, Colloidal oxide nanoparticles for the photocatalytic degradation of organic dye, Mater. Sci. Eng. C23 (2003) 285–289.
[14] V.P. Kamat, R. Huehn, R. Nicolaescu, A "sense and shoot" approach for photocatalytic degradation of organic contaminants in water, J. Phys. Chem. B 106 (2002) 788–794.
[15] S.B. Park, Y.C. Kang, Photocatalytic activity of nanometer size ZnO particles prepared by spray pyrolysis, J. Aerosol Sci. 28 (Suppl.) (1997) S473–S474.
[16] G.P. Fotou, S.E. Pratsinis, Photocatalytic destruction of phenol and salicylic acid with aerosol and commercial titania powders, Chem. Eng. Commum. 151 (1996) 251–269.
[17] M. Takagi, T. Maki, M. Miyahara, K. Mae, Productionof titania nanoparticles by using a new micro reactor assembled with same axle dual pipe, Chem. Eng. J. 101 (2004) 269–276.
[18] V. Vamathevan, R. Amal, D. Beydoun, G. Low, S. McEvoy, Silver metallisation of titania particles: effects on photoactivity forthe oxidation of organics, Chem. Eng. J. 98 (2004) 127–139.
[19] R.Y. Hong, Z.Q. Ren, J. Ding, H.Z. Li, Experimental investigation and particle dynamic simulation for synthesizing titania nano particles using diffusion flame, Chem. Eng. J. 108 (3) (2005) 203–212.
[20] D. Mondelaers, G. Vanhoyland, H. Van den Rul, J.D. Haen, M.K. Van Bael, J. Mullens, L.C. Van Poucke, Synthesis of ZnO nanopowder via an aqueous acetate–citrate gelation method, Mater. Res. Bull. 37 (2002) 901–914.
[21] M.S. Tokumoto, S.H. Pulcinelli, C.V. Santilli, V. Briois, Catalysis and temperature dependence on the formation of ZnO nanoparticles and of zinc acetate derivatives prepared by the sol–gel route, J. Phys. Chem. B 107 (2003) 568–574.
[22] T. Tsuzuki, P.G. McCormick, ZnO nanoparticles synthesized by mechanochemical processing, Scripta Mater. 44 (2001) 1731–1735.
[23] K. Okuyama, I.W. Lenggoro, Preparation of nanoparticles via spray route, Chem. Eng. Sci. 58 (2003) 537–547.
[24] F. Rataboul, C. Nayral, M.-J. Casanove, A. Maisonnat, B. Chaudret, Synthesis and characterization of monodisperse zinc and zinc oxide nanoparticles from the organometallic precursor $[Zn(C_6H_{11})_2]$, J. Organomet. Chem. 643/644 (2002) 307–312.
[25] T. Sato, T. Tanigaki, H. Suzuki, Y. Saito, O. Kido, Y. Kimura, C. Kaito, A. Takeda, S. Kaneko, Structure and optical spectrum of ZnO nanoparticles produced in RF plasma, J. Cryst. Growth 255 (2003) 313–316.
[26] R. Viswanathan, G.D. Lilly, W.F. Gale, R.B. Gupta, Formation of zinc oxide-titanium dioxide composite nanoparticles in supercritical water, Ind Eng. Chem. Res. 42 (2003) 5535–5540.
[27] Y.W. Koh, M. Lin, C.K. Tan, Y.L. Foo, K.P. Loh, Self-assembly and selected area growth of zinc oxide nanorods on any surface promoted by an aluminum precoat, J. Phys. Chem. B 108 (2004) 11419–11425.
[28] H. Zhang, D. Yang, Y. Ji, X.Y. Ma, J. Xu, D.L. Que, Low temperature synthesis of flowerlike ZnO nanostructures by cetyltrimethylammonium bromide-assisted hydro thermal process, J. Phys. Chem. B 108 (13) (2004) 3955–3958.
[29] B. Liu, H.C. Zeng, Hydrothermal synthesis of ZnO nanorods in the diameter regime of 50 nm, J. Am. Chem. Soc. 125 (2003) 4430–4431.
[30] W.D. Yu, X.M. Li, X.D. Gao, Catalytic synthesis and structural characteristics of high-quality tetrapod-like ZnO nanocrystals by a modified vapor transport process, Cryst. Growth Des. 5 (1) (2005) 151–155.
[31] X.-L. Hu, Y.-J. Zhu, S.-W. Wang, Sonochemical and microwave-assisted synthesis of linked single-crystalline ZnO rods, Mater. Chem. Phys. 88 (2004) 421–426.
[32] R.Y. Hong, Z.H. Shen, H.Z. Li, Nanosized ZnO prepared by microwave homogeneous precipitation and its photocatalytic property, Chin. J. Process Eng. 5 (6) (2005) 693–697 (in Chinese).
[33] J.M. Wang, L. Gao, Synthesis and characterization of ZnO nanoparticles assembled in one-dimensional order, Inorg. Chem. Commun. 6 (2003) 877–881.
[34] J.H. Kim, W.C. Choi, H.Y. Kim, Y. Kang, Y.-K. Park, Preparation of mono-dispersed mixed metal oxide micro hollow spheres by homogeneous precipitation in amicro precipitator, Powder Technol. 153 (2005) 166–175.

[35] R.Y. Hong, L.P. Xu, Z.Q. Ren, X. Li, H.Z. Li, Nanosized ZnO prepared by homogeneous precipitation and its photocatalytic property, Chem Eng. Environ. Protect. 25 (3) (2005) 231–234 (in Chinese).
[36] W. Posthumus, P.C.M.M. Magusin, J.C.M. Brokken-Zijp, A.H.A. Tinnemans, R. van der Linde, Surface modification of oxidic nanoparticles using 3-methacryloxypropyltrimethoxysilane, J. Colloid Interface Sci. 269 (2004) 109–116.
[37] F. Grasset, N. Saito, D. Li, D. Park, I. Sakaguchi, N. Ohashi, H. Haneda, T. Roisnel, S. Mornet, E. Duguet, Surface modification of zinc oxide nanoparticles by aminopropyltriethoxysilane, J. Alloy. Compd. 360 (2003) 298–311.
[38] B. Min, J.S. Lee, J.W. Hwang, K.H. Keem, M.I. Kang, K. Cho, M.Y. Sung, S. Kim, M.-S. Lee, S.O. Park, J.T. Moon, Al_2O_3 coating of ZnO nanorods by atomic layer deposition, J. Cryst. Growth 252 (2003) 565–569.
[39] J. H. Li, R. Y Hong, J. Wang, H. Z. Li, Comparison of different methods for preparing magnetic Fe_3O_4 nano particles, Chin. Particuol, (2006), in press.
[40] R. Y. Hong, J. Z. Qian, J. X. Cao, Synthesis and characterization of PMMA grafted ZnO nanoparticles, Powder Technol. (2006), in press.